Memorias del Congreso Nacional de Control Automático
ISSN: 2594-2492

Leader-follower formation control for mobile robots based on master-slave approach ⋆

Rigoberto Martínez-Clark * **Javier Pliego-Jiménez** ** **César Cruz-Hernandez** *

* *Electronics and Telecommunications Department, Applied Physics Division, CICESE Baja California, México*
** *Electronics and Telecommunications Department, Applied Physics Division, CICESE-CONACYT Baja California, México*

Abstract: The problem of decentralized formation control of a group of wheeled mobile robots is addressed in this paper. In order to cope with the formation control problem a strategy based on a master-slave scheme is proposed. It is assumed that only position measurements are available. Therefore, a nonlinear control algorithm in combination with velocity observer is proposed. Simulation and experimental results are presented to show the performance of the algorithm.

Keywords: Formation control, mobile robots, nonlinear control

1. INTRODUCTION

The advances achieved in robotics research of the past decades have attracted the attention in the development of multi-agent systems. Concerning to spatial distribution, one of the principal problems to solve in this scheme is formation, and many works have been reported to address it, considering different constraints and approaches (Yamaguchi et al., 2001; Wang et al., 2017; Alonso-Mora et al., 2017, and references therein).

The aim in formation control of a group of mobile robots is to drive the robots of the group to achieve and maintain a desired geometric spatial pattern (Ge and Han, 2017). A group of robots moving in formation has many advantages over a single robot performing the same tasks, for example, it can reduce the complexity of each robot; inducing to a cost reduction, also the robustness and efficiency of the systems is increased due to the redundancy and the expansion of the sensing range (Yang Quan Chen and Zhongmin Wang, 2005). This problem can be addressed as a centralized, supervisory or distributed scheme.

Formation control has broad applications, ranging from security issues like patrolling and intruder confinement, search and rescue in hostile environments, reconnaissance and combat tasks, to creation of sensor/antenna arrays, self-assembly and collective transportation, among others.

According to different control schemes, Oh et al. (2015) give a classification of formation problem as:

- Leader-follower approach: At least one robot plays the role of the leader, tracking the desired trajectory and the follower(s) robot(s) track the position of the leader to achieve formation as in (Cowan et al., 2003).
- Behavioral approach: Several desired behaviors are prescribed to the robots in this approach, including: aggregation, collision avoidance, obstacle avoidance, among others. In this approach, the formation is often amorphous, not required to show a predefined structure (see Hu et al., 2014).
- Virtual structure approach: In this approach, the robots of the group are considered as part of a single object, called a virtual structure. Therefore, the desired motion of the robots are defined by the motion of the virtual structure for example (van den Broek et al., 2009).

In this paper we apply the leader-follower approach to control a platoon of wheeled mobile robots (WMR) in order to track a predefined trajectory. As Peng et al. (2018) established, in this scheme, the interactions of the robots can be modeled with a tree topology. Considering each robot as a node and the interactions as the edges of the graph with the tree topology, one robot is designated as the root node, with the task of defining the trajectory for the whole platoon. The remaining robots, are referred as a *child* node in the tree, will reference their behaviors to their *parent* node.

⋆ This work was supported by CONACYT under Research Project **1030** "Collective behaviors of unmanned aerial and ground vehicles"

We consider the case in which the robots only have access to position measurement, therefore, a nonlinear control algorithm in combination with a velocity observer is proposed.

The remaining part of this paper is organized as follows: in Section 2 we present the kinematic model of the wheeled mobile robot and the controller design for both, the leader WMR (with a predefined trajectory tracking purpose) and the follower (which has to track the trajectory performed by the leader). In Section 3, the results of the numerical simulations are given, and lastly in Section 4 the conclusions are summarized.

2. LEADER-FOLLOWER FORMATION

The objective of this work is to achieve a leader-following formation of a group of wheeled mobile robots subject to nonholonomic constraints (see Figure 1). To this end, a master-slave approach is adopted. The master robot generates the desired trajectory for the first slave which is the nearest robot to the master. The first slave becomes the master for the second slave robot and so on (see Figure 1).

2.1 Kinematic model

Each element of the group is composed of a differential mobile robot. Let $\boldsymbol{q}_i = [\, x_i \; y_i \; \theta_i \,]^{\mathrm{T}} \in \Re^3$ be the generalized coordinates where (x_i, y_i) are the Cartesian coordinates and θ_i is the orientation angle, with $i = \{\mathrm{m}, \mathrm{s}_1, ..., \mathrm{s_n}\}$ where n is the number of slave robots. The kinematic model of the mobile robot is given by (Fierro and Lewis, 1997)

$$\dot{\boldsymbol{q}}_i = \begin{bmatrix} \cos(\theta_i) & 0 \\ \sin(\theta_i) & 0 \\ 0 & 1 \end{bmatrix} \begin{bmatrix} \nu_i \\ \omega_i \end{bmatrix} \tag{1}$$

where $\nu_i \in \Re$ and $\omega_i \in \Re$ are the linear and angular velocities of the mobile robot, respectively. In this work, a kinematic controller is developed where the linear and angular velocities are considered as the control inputs for the system (1). The orientation angle and the Cartesian velocities satisfies

$$\dot{y}_i \cos(\theta_i) - \dot{x}_i \sin(\theta_i) = 0 \tag{2}$$

or equivalently

$$\tan(\theta_i) = \frac{\dot{y}_i}{\dot{x}_i}. \tag{3}$$

The nonholonomic constraint (2) implies that the velocity in the direction of the wheel axis is zero, that is, the mobile robot cannot move in the lateral directions.

2.2 Master robot controller

It is assumed that the master tracks a desired reference trajectory given by

$$\dot{\boldsymbol{q}}_{\mathrm{r}}(t) = \begin{bmatrix} \dot{x}_{\mathrm{r}}(t) \\ \dot{y}_{\mathrm{r}}(t) \\ \dot{\theta}_{\mathrm{r}}(t) \end{bmatrix} = \begin{bmatrix} \cos(\theta_{\mathrm{r}}(t)) & 0 \\ \sin(\theta_{\mathrm{r}}(t)) & 0 \\ 0 & 1 \end{bmatrix} \begin{bmatrix} \nu_{\mathrm{r}}(t) \\ \omega_{\mathrm{r}}(t) \end{bmatrix} \tag{4}$$

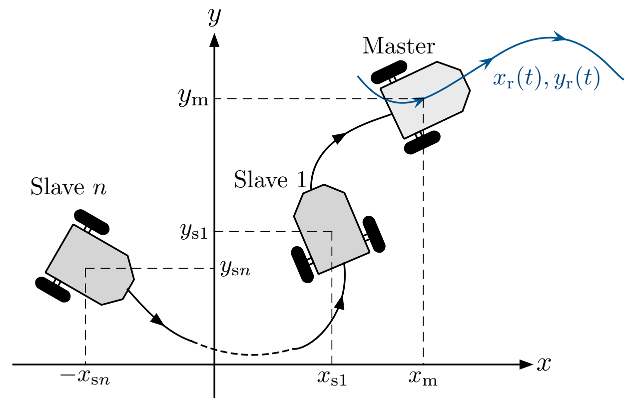

Fig. 1. Formation of a group of mobile robots

where $\nu_{\mathrm{r}}(t)$ and $\omega_{\mathrm{r}}(t)$ are continuous functions of t. To avoid solving the differential equation (4) we can use the fact that the system (4) is differentially flat (Luviano-Juarez et al., 2015). Taking the Cartesian coordinates $x_{\mathrm{r}}(t)$ and $y_{\mathrm{r}}(t)$ as the flats outputs we can express any variable of (4) as a function of the flat outputs and a finite number of their derivatives,

$$\left.\begin{aligned} \theta_{\mathrm{r}}(t) &= \tan^{-1}\left(\frac{\dot{x}_{\mathrm{r}}}{\dot{y}_{\mathrm{r}}}\right) \\ \nu_{\mathrm{r}}(t) &= \sqrt{\dot{x}_{\mathrm{r}}(t) + \dot{y}_{\mathrm{r}}(t)} \\ \omega_{\mathrm{r}}(t) &= \frac{\dot{x}_{\mathrm{r}}\ddot{y}_{\mathrm{r}} - \dot{y}_{\mathrm{r}}\ddot{x}_{\mathrm{r}}}{\dot{x}_{\mathrm{r}}^2 + \dot{y}_{\mathrm{r}}^2} \end{aligned}\right\} \tag{5}$$

for any continuously differentiable and bounded functions $x_{\mathrm{r}}(t)$ and $y_{\mathrm{r}}(t)$. For control design purposes we define the following continuous function

$$\phi(\vartheta) = |\vartheta|^{\alpha} \operatorname{sign}(\vartheta), \quad \forall \vartheta \in \Re \tag{6}$$

where $0 < \alpha \leq 1$, if $\alpha = 1$ we have $\phi(\vartheta) = \vartheta$. The function $\phi(\vartheta)$ satisfies

$$\vartheta\phi(\vartheta) > 0, \quad \forall \vartheta \neq 0. \tag{7}$$

Notice that $\frac{\mathrm{d}}{\mathrm{d}t}(\vartheta\phi(\vartheta))$ is also a continuous function. In order to develop a control algorithm for the master robot the tracking error is defined as

$$\boldsymbol{e}_{\mathrm{m}} \triangleq \boldsymbol{q}_{\mathrm{r}}(t) - \boldsymbol{q}_{\mathrm{m}} = \begin{bmatrix} x_{\mathrm{r}}(t) - x_{\mathrm{m}} \\ y_{\mathrm{r}}(t) - y_{\mathrm{m}} \\ \theta_{\mathrm{r}}(t) - \theta_{\mathrm{m}} \end{bmatrix} \tag{8}$$

Consider the change of coordinates (Fierro and Lewis, 1997)

$$\boldsymbol{\xi}_{\mathrm{m}} = \begin{bmatrix} \cos(\theta_{\mathrm{m}}) & \sin(\theta_{\mathrm{m}}) & 0 \\ -\sin(\theta_{\mathrm{m}}) & \cos(\theta_{\mathrm{m}}) & 0 \\ 0 & 0 & 1 \end{bmatrix} \boldsymbol{e}_{\mathrm{m}} = \boldsymbol{R}(\theta_{\mathrm{m}})\boldsymbol{e}_{\mathrm{m}} \tag{9}$$

where $\boldsymbol{R}(\theta_{\mathrm{m}})$ is an orthogonal matrix. By taking into account equations (1) and (4) the open-loop error dynamics of the master in the new coordinates is described by

$$\dot{\boldsymbol{\xi}}_{\mathrm{m}} = \begin{bmatrix} \nu_{\mathrm{r}}(t)\cos(\xi_{\mathrm{m}3}) + \xi_{\mathrm{m}2}\omega_{\mathrm{m}} - \nu_{\mathrm{m}} \\ \nu_{\mathrm{r}}(t)\sin(\xi_{\mathrm{m}3}) - \xi_{\mathrm{m}1}\omega_{\mathrm{m}} \\ \omega_{\mathrm{r}}(t) - \omega_{\mathrm{m}} \end{bmatrix}. \tag{10}$$

where $\boldsymbol{\xi}_{\mathrm{m}} = [\, \xi_{\mathrm{m}1} \; \xi_{\mathrm{m}2} \; \xi_{\mathrm{m}2} \,]^{\mathrm{T}}$.

Based on (Kostic et al., 2009) the proposed control algorithm for the master is given by

$$\nu_{\rm m} = k_{\rm m1}\phi(\xi_{\rm m1}) + \nu_{\rm r}(t)\cos(\xi_{\rm m3}) \quad (11)$$

$$\omega_{\rm m} = \kappa_{\rm m} k_{\rm m2}\frac{\sin(\xi_{\rm m3})\xi_{\rm m2}\nu_{\rm r}(t)}{\xi_{\rm m3}\sqrt{1+\kappa_{\rm m}^2\|\boldsymbol{\xi}_{\rm pm}\|^2}} + k_{\rm m3}\phi(\xi_{\rm m3}) + \omega_{\rm r}(t) \quad (12)$$

where $\kappa_{\rm m}, k_{\rm m1}, k_{\rm m2}$ and $k_{\rm m3} \in \Re$ are positive control gains and $\boldsymbol{\xi}_{\rm pm} = \left[\,\xi_{\rm m1}\ \xi_{\rm m2}\,\right]^{\rm T}$. The controller (11) and (12) in closed-loop with (10) yields

$$\dot{\boldsymbol{\xi}}_{\rm m} = \begin{bmatrix} -k_{\rm m1}\phi(\xi_{\rm m1}) + \xi_{\rm m2}\omega_{\rm m} \\ \nu_{\rm r}\sin(\xi_{\rm m3}) - \xi_{\rm m1}\omega_{\rm m} \\ -k_{\rm m3}\phi(\xi_{\rm m3}) - \dfrac{\sin(\xi_{\rm m3})}{\xi_{\rm m3}}\cdot\dfrac{\kappa_{\rm m}k_{\rm m2}\nu_{\rm r}(t)\xi_{\rm m2}}{\sqrt{1+\kappa_{\rm m}\|\boldsymbol{\xi}_{\rm pm}\|^2}} \end{bmatrix} \quad (13)$$

The above equation describe the closed-loop error dynamics of the master. Since

$$\lim_{\xi_{\rm m3}\to 0}\frac{\sin(\xi_{\rm m3})}{\xi_{\rm m3}} = 1$$

the differential equation (13) has an equilibrium point at $\boldsymbol{\xi}_{\rm m} = \mathbf{0}$. For stability analysis consider the following lemma

Lemma 1. (Jiang and Nijmeijer (1997)). Consider a scalar system

$$\dot{x} = -cx + \rho(t)$$

where $c > 0$ and $\rho(t)$ is bounded and uniformly continuous function. If, for any time $t_0 \geq 0$ and any initial condition $x(t_0) = x_0$, the solution $x(t)$ asymptotically converge to zero then

$$\lim_{t\to\infty}\rho(t) = 0$$

△

Theorem 1. Suppose that $\nu_{\rm r}(t)$ does not converge to zero, then the proposed controller for the master robot given in (11)-(12) guarantees that the tracking error $\boldsymbol{e}_{\rm m}$ defined in (8) converge to zero as $t \to \infty$.

Proof. From equation (9) we have $\boldsymbol{e}_{\rm m} = \boldsymbol{R}^{\rm T}(\theta_{\rm m})\boldsymbol{\xi}_{\rm m}$. Therefore, in order to prove that $\boldsymbol{e}_{\rm m} \to \mathbf{0}$ as $t \to \infty$ it is only necessary to prove that $\boldsymbol{\xi}_{\rm m}$ converges asymptotically to zero. To this end, consider the scalar positive definite function

$$V_{\rm m} = \frac{k_{\rm m2}}{\kappa_{\rm m}}\left(\sqrt{1+\kappa^2\|\boldsymbol{\xi}_{\rm pm}\|^2} - 1\right) + \frac{1}{2}\xi_{\rm m3}^2 \quad (14)$$

whose derivative along (13) is given by

$$\dot{V}_{\rm m} = -k_{\rm m}^{\star}\frac{\xi_{\rm m1}\phi(\xi_{\rm m1})}{\sqrt{1+k^2\|\boldsymbol{\xi}_{\rm pm}\|^2}} - k_{\rm m3}\xi_{\rm m3}\phi(\xi_{\rm m3}) \leq 0 \quad (15)$$

where $k_{\rm m}^{\star} \triangleq \kappa_{\rm m}k_{\rm m1}k_{\rm m2}$. Since the derivative of $V_{\rm m}$ is negative semidefinite the tracking errors are bounded, *i.e.*, $\boldsymbol{\xi}_{\mathbf{m}}, \boldsymbol{e}_{\rm m} \in \mathcal{L}_\infty$. By applying Barbalt's lemma it is straight forward to prove that $\xi_{\rm m1}$ and $\xi_{\rm m3}$ converge asymptotically to zero.

Let us analyze the differential equation $\dot{\xi}_{\rm m3}$

$$\dot{\xi}_{\rm m3} = -k_{\rm m3}\phi(\xi_{\rm m3}) - \underbrace{\kappa_{\rm m}k_{\rm m2}\frac{\sin(\xi_{\rm m3})}{\xi_{\rm m3}}\cdot\frac{\nu_{\rm r}(t)\xi_{\rm m2}}{\sqrt{1+k\|\boldsymbol{\xi}_{\rm pm}\|^2}}}_{\rho(t)}$$

According to Lemma 1 we have

$$\lim_{t\to\infty}\rho(t) = \kappa_{\rm m}k_{\rm m2}\frac{\sin(\xi_{\rm m3})}{\xi_{\rm m3}}\cdot\frac{\nu_{\rm r}(t)\xi_{\rm m2}}{\sqrt{1+k\|\boldsymbol{\xi}_{\rm pm}\|^2}} = 0$$

Since $\sin(\xi_{\rm m3})/\xi_{\rm m3} \to 1$ as $\xi_{\rm m3} \to 0$ we concluded that $\xi_{\rm m2}$ converges asymptotically to zero whether $\nu_{\rm r}(t)$ does not converge to zero. △

2.3 Slave controller

In the master-slave scheme the desired trajectory for the slave robot is generated by the master. In this work, it is assumed that only the robots' position is available from measurements. Thus, a Luenberger-like observer is proposed to estimate the velocity of the master,

$$\dot{\widehat{\boldsymbol{q}}}_{\rm m} = \boldsymbol{G}_{\rm m}(\boldsymbol{q}_{\rm m})\boldsymbol{\nu}_{\rm m} - \boldsymbol{\Lambda}_1\widetilde{\boldsymbol{q}}_{\rm m} - \boldsymbol{\Lambda}_2\boldsymbol{\sigma}_{\rm m} \quad (16)$$

$$\dot{\boldsymbol{\sigma}}_{\rm m} = \widetilde{\boldsymbol{q}}_{\rm m} \quad (17)$$

$$\widetilde{\boldsymbol{q}}_{\rm m} = \widehat{\boldsymbol{q}}_{\rm m} - \boldsymbol{q}_{\rm m} \quad (18)$$

where $\widehat{\boldsymbol{q}}_{\rm m} = \left[\,\widehat{x}_{\rm m}\ \widehat{y}_{\rm m}\ \widehat{\theta}_{\rm m}\,\right]^{\rm T} \in \Re^3$ is an estimate of $\boldsymbol{q}_{\rm m}$, $\boldsymbol{\Lambda}_1$ and $\boldsymbol{\Lambda}_2 \in \Re^{3\times 3}$ are diagonal positive definite matrices and

$$\boldsymbol{G}_{\rm m}(\boldsymbol{q}_{\rm m}) = \begin{bmatrix}\cos(\theta_{\rm m}) & 0 \\ \sin(\theta_{\rm m}) & 0 \\ 0 & 1\end{bmatrix}, \quad \boldsymbol{\nu}_{\rm m} = \begin{bmatrix}\nu_{\rm m} \\ \omega_{\rm m}\end{bmatrix}$$

By taking into account (1) and (16) the derivative of the estimation error $\widetilde{\boldsymbol{q}}_{\rm m}$ with respect to time is given by

$$\dot{\widetilde{\boldsymbol{q}}}_{\rm m} = \dot{\widehat{\boldsymbol{q}}}_{\rm m} - \dot{\boldsymbol{q}}_{\rm m} = -\boldsymbol{\Lambda}_1\widetilde{\boldsymbol{q}}_{\rm m} - \boldsymbol{\Lambda}_2\boldsymbol{\sigma}_{\rm m}. \quad (19)$$

Differentiating once again the estimation error leads to

$$\ddot{\widetilde{\boldsymbol{q}}}_{\rm m} + \boldsymbol{\Lambda}_1\dot{\widetilde{\boldsymbol{q}}}_{\rm m} + \boldsymbol{\Lambda}_2\widetilde{\boldsymbol{q}}_{\rm m} = \mathbf{0}. \quad (20)$$

The foregoing equation can be expressed as follows

$$\frac{\rm d}{{\rm d}t}\begin{bmatrix}\widetilde{\boldsymbol{q}}_{\rm m} \\ \dot{\widetilde{\boldsymbol{q}}}_{\rm m}\end{bmatrix} = \begin{bmatrix}\boldsymbol{O} & \boldsymbol{I} \\ -\boldsymbol{\Lambda}_1 & -\boldsymbol{\Lambda}_2\end{bmatrix}\begin{bmatrix}\widetilde{\boldsymbol{q}}_{\rm m} \\ \dot{\widetilde{\boldsymbol{q}}}_{\rm m}\end{bmatrix} = \boldsymbol{A}\begin{bmatrix}\widetilde{\boldsymbol{q}}_{\rm m} \\ \dot{\widetilde{\boldsymbol{q}}}_{\rm m}\end{bmatrix}$$

The observer gains can be chosen such that the matrix $\boldsymbol{A} \in \Re^{6\times 6}$ is Hurwitz. Therefore, the estimation error $\widetilde{\boldsymbol{q}}_{\rm m}$ and its derivative $\dot{\widetilde{\boldsymbol{q}}}_{\rm m}$ converge asymptotically to zero. This in turn implies $\dot{\widehat{\boldsymbol{q}}}_{\rm m} \to \dot{\boldsymbol{q}}_{\rm m}$ as $t \to \infty$.

Once the velocity observer has been developed the next step is to design the tracking controller for the slave mobile robot. Similar to (8) and (9) the slave errors are defined as

$$\boldsymbol{\xi}_{\rm s} = \boldsymbol{R}(\theta_{\rm s})\boldsymbol{e}_{\rm s}, \quad \boldsymbol{e}_{\rm s} = \begin{bmatrix}x_{\rm m}(t-T) - x_{\rm s} \\ y_{\rm m}(t-T) - y_{\rm s} \\ \theta_{\rm m}(t-T) - \theta_{\rm s}\end{bmatrix} \quad (21)$$

where $T > 0$ is a constant time delay. The proposed controller for the slave is given by

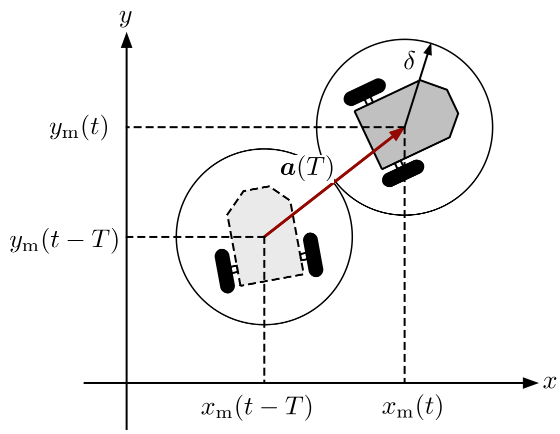

Fig. 2. Collision avoidance

$$\nu_{\mathrm{s}} = k_{\mathrm{s}1}\phi(\xi_{\mathrm{s}1}) + \nu_{\mathrm{rm}}(t)\cos(\xi_{\mathrm{s}3}) \tag{22}$$

$$\omega_{\mathrm{s}} = \kappa_{\mathrm{s}} k_{\mathrm{s}2} \frac{\sin(\xi_{\mathrm{s}3})\xi_{\mathrm{m}2}\nu_{\mathrm{rm}}(t)}{\xi_{\mathrm{s}3}\sqrt{1+\kappa_{\mathrm{s}}^2\|\boldsymbol{\xi}_{\mathrm{ps}}\|^2}} + k_{\mathrm{s}3}\phi(\xi_{\mathrm{s}3}) + \omega_{\mathrm{rm}}(t) \tag{23}$$

where κ_{s}, $k_{\mathrm{s}1}$,$k_{\mathrm{s}2}$, $k_{\mathrm{s}3}$ $\in \Re$ are positive control gains, $\boldsymbol{\xi}_{\mathrm{ps}} = [\,\xi_{\mathrm{s}1}\ \ \xi_{\mathrm{s}2}\,]^{\mathrm{T}}$ and

$$\nu_{\mathrm{rm}}(t) = \sqrt{\dot{\hat{x}}_{\mathrm{m}}^2(t-T) + \dot{\hat{y}}_{\mathrm{m}}^2(t-T)}$$
$$\omega_{\mathrm{rm}}(t) = \dot{\hat{\theta}}_{\mathrm{m}}(t-T).$$

Theorem 2. Suppose that $v_{\mathrm{rm}}(t)$ does not converge to zero then the control algorithms for the slave robot given in (22) and (23) guarantee that the slave tracking error converges asymptotically to zero. △

The proof of Theorem 2 is similar to the proof of Theorem 1 and hence is omitted. In order to avoid collision between robots, the time-delay T can be chosen such that

$$\|\boldsymbol{a}(T)\| > 2\delta$$

where $\boldsymbol{a}(T) = [\,x_{\mathrm{m}}(t) - x_{\mathrm{m}}(t-T)\ \ y_{\mathrm{m}}(t) - y_{\mathrm{m}}(t-T)\,]^{\mathrm{T}}$ and $\delta > 0$ is the radius of a virtual circle that encloses the robot (see Figure 2).

Robot	Controller	Observer
Master	$\boldsymbol{K}_{\mathrm{m}} = \begin{bmatrix} 1.7 & 0 & 0 \\ 0 & 1.7 & 0 \\ 0 & 0 & 1.20 \end{bmatrix}$	$\boldsymbol{\Lambda}_1 = 2\boldsymbol{I}$, $\boldsymbol{\Lambda}_2 = \boldsymbol{I}$
Slave 1	$\boldsymbol{K}_{\mathrm{s}} = \begin{bmatrix} 1.5 & 0 & 0 \\ 0 & 2.0 & 0 \\ 0 & 0 & 0.35 \end{bmatrix}$	$\boldsymbol{\Lambda}_1 = 4\boldsymbol{I}$, $\boldsymbol{\Lambda}_2 = 2\boldsymbol{I}$
Slave 2	$\boldsymbol{K}_{\mathrm{s}} = \begin{bmatrix} 1.5 & 0 & 0 \\ 0 & 1.5 & 0 \\ 0 & 0 & 0.25 \end{bmatrix}$	-

Table 1. Controller and observer gains used in simulations

3. SIMULATIONS

Simulations were carried out to assess the performance of the proposed controller and velocity observer. The group is composed of three mobile robots. In the simulation the first slave becomes the master for the second slave robot. The reference trajectory for the master robot is given by

$$x_{\mathrm{r}}(t) = \sin\left(\frac{t}{5}\right)\,[\mathrm{m}], \quad y_{\mathrm{r}}(t) = \sin\left(\frac{t}{10}\right)\,[\mathrm{m}]$$

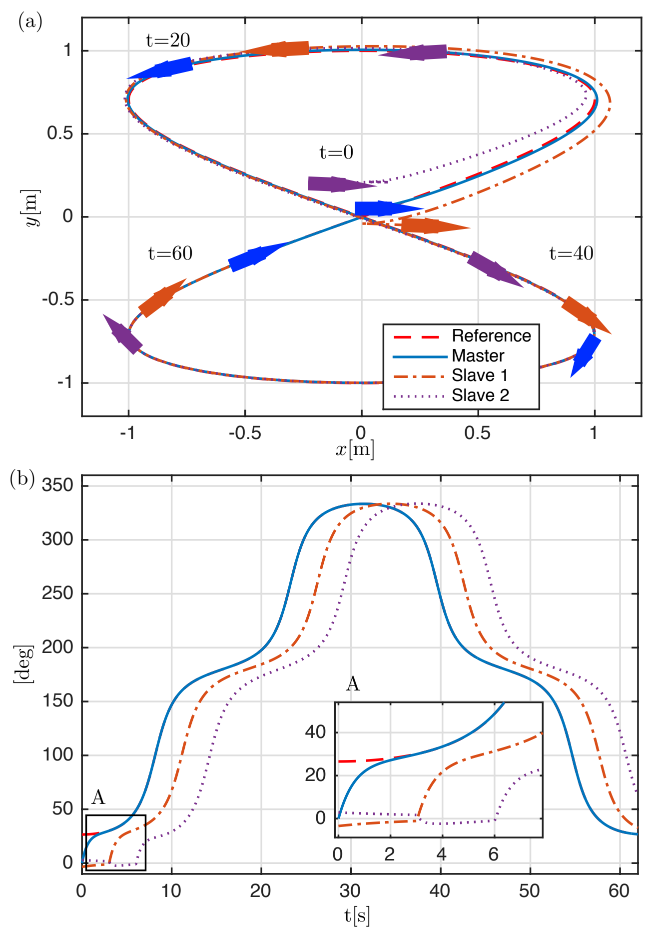

Fig. 3. Trajectory of the object, (a) Cartesian coordinates and (b) orientation

The time delay is set to $T = 3$[s]. The controller and observer gains used in simulations are shown in Table 1 where $\boldsymbol{K}_{\mathrm{m}} = \mathrm{diag}\{k_{\mathrm{m}1}, k_{\mathrm{m}2}, k_{\mathrm{m}3}\}$ and $\boldsymbol{K}_{\mathrm{s}} = \mathrm{diag}\{k_{\mathrm{s}1}, k_{\mathrm{s}2}, k_{\mathrm{s}3}\}$. The Cartesian trajectory of the robots and their orientation are shown in Figure 3. The figure also shows the position of the robots at time instants $t = 0$, $t = 20$, $t = 40$ and $t = 60$ seconds. We recall that the first slave becomes the master for the for the second robot. The tracking errors are shown in Figure 4. The observation errors are shown in Figure 5. In both cases, the tracking and observation errors converge asymptotically to zero. Finally, Figure 6 shows the control inputs. Notice that the initial position errors for the second slave

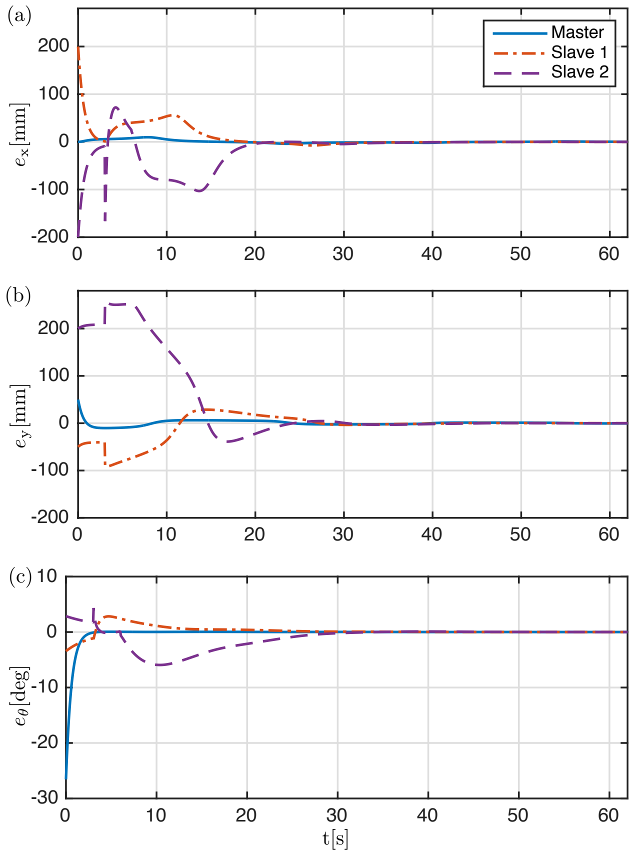

Fig. 4. Tracking errors, (a) e_{xj} (b) e_{yj} and (c) $e_{\theta j}$

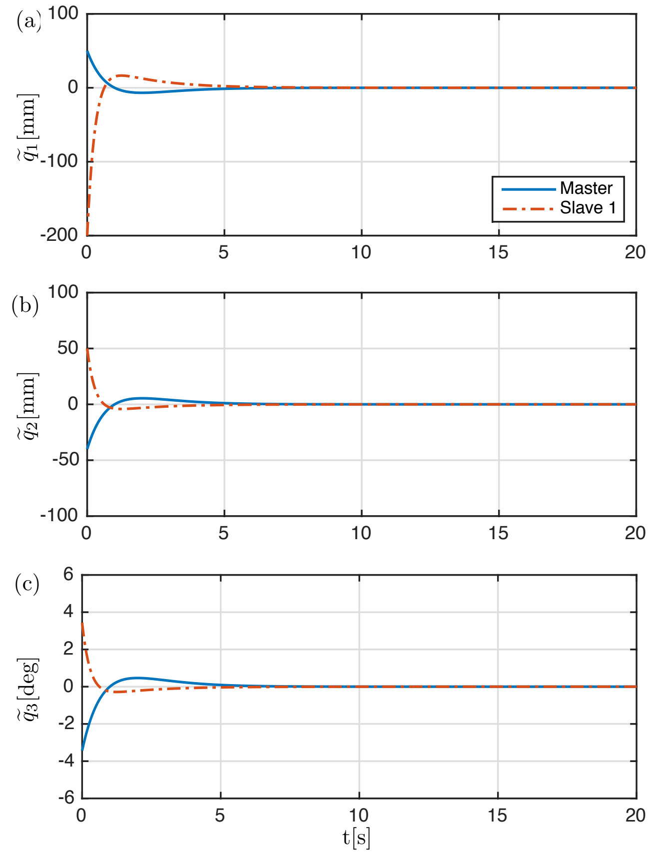

Fig. 5. Observation errors, (a) $\widetilde{q}_1 = \widehat{x} - x$ (b) $\widetilde{q}_2 = \widehat{y} - y$ and (c) $\widetilde{q}_3 = \widehat{\theta} - \theta$

are bigger than the master and first slave errors. Consequently, the second slave requires more control effort at the beginning of the trajectory.

4. CONCLUSIONS

In this article, we addressed the problem of formation control of a group of wheeled mobile robots. The proposed approach is based on a master-slave scheme, to avoid collisions the slave robot follows the delay trajectory of the master. In order to achieve trajectory tracking with only position measurements a kinematic nonlinear controller and velocity observer are proposed. The performance of the controller and observer is evaluated by means of numerical simulations. Experimental validation of the proposed approach and designing a tracking controller and observer that take into account the dynamic model of the mobile robots are considered as a future work.

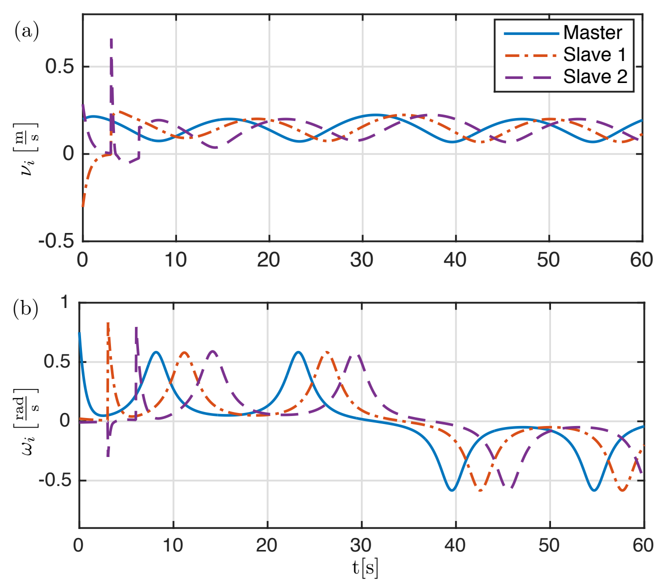

Fig. 6. Control inputs, (a) ν_i and (b) ω_i

REFERENCES

Alonso-Mora, J., Baker, S., and Rus, D. (2017). Multi-robot formation control and object transport in dynamic environments via constrained optimization. *The International Journal of Robotics Research*, 36(9), 1000–1021.

Cowan, N., Shakerina, O., Vidal, R., and Sastry, S. (2003). Vision-based follow-the-leader. In *Proceedings 2003 IEEE/RSJ International Conference on Intelligent Robots and Systems (IROS 2003)*, volume 2, 1796–1801. IEEE.

Fierro, R. and Lewis, F. (1997). Control of a nonholonomic mobile robot: Backstepping kinematics into dynamics. *Journal of Robotic Systems*, 14(3), 149–163.

Ge, X. and Han, Q.L. (2017). Distributed Formation Control of Networked Multi-Agent Systems Using a Dynamic Event-Triggered Communication Mechanism. *IEEE Transactions on Industrial Electronics*, 64(10), 8118–8127.

Hu, D., Zhong, M., Zhang, X., and Yao, Y. (2014). Self-Organized Aggregation Based on Cockroach Behavior in Swarm Robotics. *2014 Sixth International Conference on Intelligent Human-Machine Systems and Cybernetics*, 349–354.

Jiang, Z. and Nijmeijer, H. (1997). Tracking control of mobile robots: a case study in backstepping. *Automatica*, 33(7), 1393–1399.

Kostic, D., Adinandra, S., Caarls, J., van de Wouw, N., and Nijmeijer, H. (2009). Collision-free tracking control of unicycle mobile robots. In *Conference on Decision and Control*, 5667–5672.

Luviano-Juarez, A., Cortes-Romero, J., and Sira-Ramirez, H. (2015). Trajectory tracking control of a mobile robot through a flatness-based exact feedforward linearization scheme. *Journal of Dynamic Systems Measurement and Control*, 137(5), 1–8.

Oh, K.K., Park, M.C., and Ahn, H.S. (2015). A survey of multi-agent formation control. *Automatica*, 53, 424–440.

Peng, L., Guan, F., Perneel, L., Fayyad-Kazan, H., and Timmerman, M. (2018). Decentralized Multi-Robot Formation Control with Communication Delay and Asynchronous Clock. *Journal of Intelligent & Robotic Systems*, 89(3-4), 465–484.

van den Broek, T.H., van de Wouw, N., and Nijmeijer, H. (2009). Formation control of unicycle mobile robots: a virtual structure approach. In *Proceedings of the 48h IEEE Conference on Decision and Control (CDC) held jointly with 2009 28th Chinese Control Conference*, 8328–8333. IEEE.

Wang, Q., Chen, Z., Liu, P., and Hua, Q. (2017). Distributed multi-robot formation control in switching networks. *Neurocomputing*, 270, 4–10.

Yamaguchi, H., Arai, T., and Beni, G. (2001). A distributed control scheme for multiple robotic vehicles to make group formations. *Robotics and Autonomous Systems*, 36(4), 125–147.

Yang Quan Chen and Zhongmin Wang (2005). Formation control: a review and a new consideration. In *2005 IEEE/RSJ International Conference on Intelligent Robots and Systems*, 3181–3186. IEEE.

